OPTICS11

WHITE PAPER



CONTACT INFORMATION
Optics11
+31 20 598 7917
info@optics11.com
www.optics11.com

VISITING ADRESS
Optics11
VU University Campus
W&N Building room O-236
De Boelelaan 1081
1081 HV Amsterdam
The Netherlands

SHIPPING ADRESS
Optics11
De Boelelaan 1081
1081 HV Amsterdam
The Netherlands

COMPANY INFORMATION
Optics11 B.V.
KvK/CC: 52469417
VAT: NL850459734B01
Amsterdam, NL

Optics11 Piuma White Paper. Published October 2017.

Please see our website for more information about our products

Measuring micro-mechanical properties of (bio)materials by nano-indentation

Measuring micro-mechanical properties of (bio)materials by nano-indentation

G. Mattei, N. Looze, E.J. Breel – August 2017, Optics11 B.V., Amsterdam, NL

Mechanical properties are important parameters in the characterisation of materials for many disciplines in science and engineering. They provide direct information about material behaviour, quality or performance. Characterising material mechanical behaviour, particularly at typical cell length scales, is becoming increasingly important in the fields of biomaterial engineering and tissue engineering. Mainly because the mechanical properties of cell micro-environment are known to play critical roles in regulating cell function and behaviour through mechano-transduction mechanisms. Among available mechanical testing techniques, nano-indentation is well suited and widely used to characterise the micro-mechanical properties of biological tissues and (bio)materials. This whitepaper describes the important aspects of nano-indentation and summarises the most common modelling and interpretation of nano-indentation data.

1. Introduction

Tensile and compression tests, indentation, shear rheometry, dynamic mechanical analysis and ultrasound-based approaches are only a few examples of methods to determine either bulk or local material mechanical properties [1]. Among these methods, nano-indentation is an emerging technology for the mechanical characterisation of biological tissues and (bio)materials for several reasons [2,3]. First of all, this method is capable of local (small scale) indentation and therefore allows to assess the heterogeneity of materials. It enables to investigate their hierarchical multi-scale organisation [4]. In contrast to most classical methods, it does not require extensive sample preparation prior to testing. Furthermore, nano-indentation allows the measurement of very small
forces and displacements, generally in the range of µN–mN and nm–µm, respectively [5]. Nano-indentation methods requires small volumes of materials, making it particularly suitable for valuable samples [6]. Additionally, a broad variety of deformation modes can be studied by changing experimental time scales, indenter tip geometry and loading conditions. Because nano-indentation applies very small forces on a sample, the technique is well suited for soft biomaterials [7] such as hydrogels [8]. Due to the pliable and highly hydrated nature of hydrogels, they are a challenge to characterise using macro-scale techniques. Finally, this method can be also attractive in the biomedical context for smart scaffold design or as a potential diagnostic tool [9], given that the mechanical properties of cell micro-environment are known to play critical roles in regulating (patho)physiological cell function and behaviour via mechano-transduction [10–12] and since pathological and ageing tissues are known to exhibit altered mechanical properties [1].

Typically, an indentation test starts when the indenter probe is out of contact, slightly above

the surface of the sample. The latter is then approached until the tip of the indenter enters in contact with it. At this point the loading phase begins (Fig. 1). The sample is being pressed by the indentation probe while load (P) and surface displacement (or indentation, h) are recorded.

Commercial nano-indenters can be operated either in load- (i.e. controlling the force applied to the sample) or indentation-control mode (i.e. controlling the surface displacement during testing). It uses load-based contact determination methods that measures either a small force on the sample or a small change in the apparent stiffness by an instantaneous reading of $S = \partial P/\partial h$ (Fig. 1) [13]. The majority of nano-indenters are equipped with an automated x–y stage that allows several measurements over the surface of the sample and spatial mapping of its local mechanical properties [14]. When the maximum load or indentation depth is reached, as set by the user, the unloading phase starts, and the indenter tip begins to retract. The moment at which the tip loses contact with the sample, the unloading phase ends and the indentation cycle is completed.

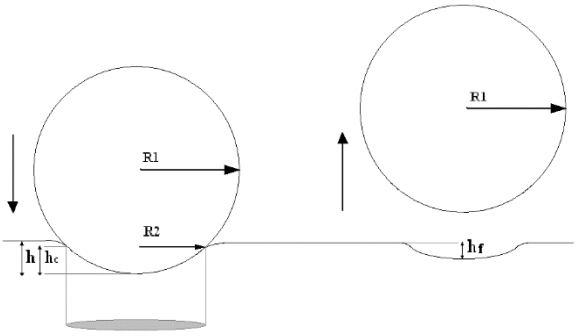

Figure 1 – Schematic representation of sample indentation with a spherical indenter tip.

During the approaching phase, zero load is measured with increasing displacement. The loading phase starts after reaching the contact point. Sometimes, a negative load can be recorded at this stage due to pull-on adhesion forces pulling down the indenter tip: a phenomenon called "snap-in". Most reports define the point of contact as the position on the loading curve at which the tip snaps into contact [15]. However, the snap into contact may be not clearly visible on load-displacement curve when testing soft biological tissues or hydrogels, requiring other definitions to identify the contact point.

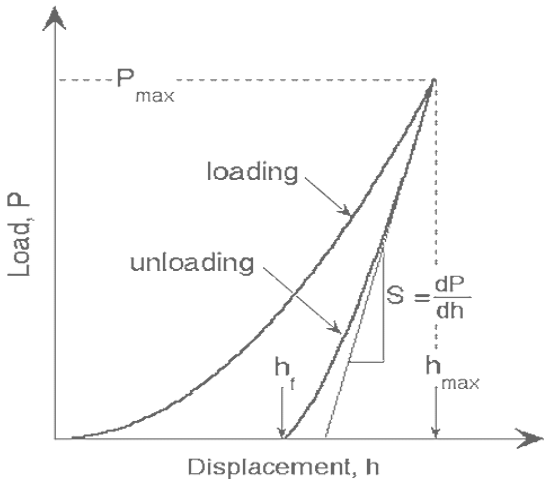

Figure 2 – load-displacement curve

Kaufman et al. proposed to determine the contact point as the point of lowest force on the unloading curve [16]. Other studies, define the contact point as the last point at which the load crosses the abscissa of the load-displacement curve during loading [3,17,18]. This definition allows a unique identification of the initial point of contact even when the snap into contact is not clearly evident or in the presence of noise around zero load. A load- or displacement-holding phase (dependent on the indenter control-mode) can be set in between the loading and the unloading phase in order to investigate eventual sample creep or stress relaxation (see section 3). The displacement holding phase is shown at the end of the loading curve in figure 1. After, the unloading phase starts and again a negative load can be recorded due to adhesion forces between indenter tip and material surface, a phenomenon called "snap-out". The load-indentation cycle terminates when the indenter tip loses contact with the sample surface. The experimental $P - h$ data recorded over time (t) (Fig. 2) are then analysed with a range of models to derive material mechanical properties. Examples of mechanical parameters that can be derived are elastic, elastoplastic, viscoelastic or poro-viscoelastic [19]. Before performing indentation tests, one has to be aware of a few factors that may play a significant role in the outcome of measurements.

For example, the effective contact area of the indenter tip depends strongly on the surface roughness and topography of the sample. Therefore, to avoid errors, it is important to work with well defined, locally flat samples. The sample has to be properly fixed to avoid any lateral movement during indentation. It also has to have an appropriate thickness, which is typically more than ten times the desired indentation depth. In this way, one can be sure that the properties of the substrate will not significantly influence the result of the measurement. These are only few examples of factors that have to be considered before the experiment. Some specimens may need a more elaborate approach that requires a deeper thought on viscoelastic effects or adhesion forces. Therefore, basic knowledge about the sample is necessary to avoid major errors in the estimation of its mechanical properties.
The following sections aim to provide a practical overview on some of the most widely used methods to derive either elastic or viscoelastic micro-mechanical properties on nano-indentation data acquired using a spherical probe.

2. Elastic properties

Unloading curve analysis: the Oliver-Pharr model

Oliver and Pharr model, introduced in 1992 [20] and revised in 2004 [21], is based on an elastic–plastic contact model and uses three key parameters from the indentation test, namely the peak indenter force (P_{max}), the peak indenter displacement (h_{max}), the unloading slope or stiffness ($S = \partial P/\partial h$) (Fig. 1). Additionally, it uses the final indentation depth (h_f) and contact depth (h_c) to derive the contact radius. The equations in this model for a spherical indenter are given by:

$$P = \frac{4}{3}\sqrt{(R)} \cdot E \cdot (h - hf)^{3/2} \quad (1)$$

$$S = \frac{\Delta P}{\Delta h} = 2\sqrt{(R)} \cdot E \cdot (h - hf)^{1/2} \quad (2)$$

$$\frac{1}{R} = (\frac{1}{R1} + \frac{1}{R2})^{-1} \quad (3)$$

The radius used in this method (R) is the effective radius and, as suggested by equation 3, comes from the combination of the indenter radius (R_1) and the contact radius (R_2). It is difficult to directly measure the contact radius during experiments. Alternatively, the contact radius can be approximated by calculating the contact depth (h_c) with the help of the measured maximum displacement (h_{max}) and final displacement (h_f):

$$h_c = h_{max} - \frac{\epsilon \cdot P_{max}}{S} \quad (4)$$

ϵ=0.75 for a spherical indenter

$$h_c = \frac{h_{max} - h_f}{2} \quad (5)$$

Loading curve analysis: the Hertz model

The use of the loading portion of the load-displacement curve, instead of the classical unloading portion used in the Oliver–Pharr approach, is far more suitable for soft samples like biological tissues and (bio)materials. In particular, the mechanical properties derived from the loading portion of the curve are representative of those of the virgin material, returning a constant modulus value regardless of the maximum load (or displacement) chosen for the measurements. Conversely, the modulus value obtained from the unloading curve is likely to increase with increasing maximum indentation load (or displacement), as expected when going beyond the sample linear elastic (or viscoelastic) region [22]. Moreover, during unloading it is assumed that only the elastic displacements are recovered [21], thus methods based on the unloading curve are unsuitable for testing viscoelastic materials.
The analysis of the loading part of nano-indentation data collected with a spherical tip is generally based on the Hertz model (Fig. 2), assuming a linear elastic and isotropic material response [23]. The load P is expressed as:

$$P = \frac{4}{3} E_{eff} R^{1/2} h^{3/2} \quad (6)$$

where R is the radius of the spherical indenter tip, h is the penetration depth and E_{eff} denotes the effective composite elastic modulus of the indenter and specimen system given by:

$$\frac{1}{E_{eff}} = \frac{1-\upsilon^2}{E} + \frac{1-\upsilon'^2}{E'} \quad (7)$$

In Eq. 7, E' and υ' respectively refer to the modulus and Poisson's ratio of the indenter, while the other terms refer to those of the sample. For a rigid spherical indenter, Sneddon [24] showed that the elastic displacements of a plane surface above and below the circle of contact are equal and given by $h/2$, with:

$$h = \frac{a^2}{R} \quad (8)$$

where a denotes the contact radius during indentation (Fig. 2). Combining Eqs. 1 and 3 yields:

$$\frac{P}{\pi a^2} = \frac{4}{3\pi} E_{eff} \left(\frac{a}{R}\right) \quad (9)$$

The left side of Eq. 9 is referred to as the indentation stress (σ_{ind}) or mean contact pressure, while a/R on the right side represents the indentation strain (ε_{ind}) [25].
In case of soft materials, where $E' \gg E$, Eq. 7 can be approximated as follows:

$$\frac{1}{E_{eff}} \approx \frac{1-\upsilon^2}{E} \quad (10)$$

Consequently, the sample elastic modulus can be derived as:

$$E = \frac{3(1-\upsilon^2)P}{4R^{1/2}h^{3/2}} \quad (11)$$

3. Viscoelastic properties

Creep

A creep test is based on applying a constant load and measuring the change in displacement over time due to viscoelastic phenomena. Hertz-type viscoelastic theory can be used to obtain the equivalent creep compliance of a material under a step load (P_0, constant over time) imposed by a spherical indenter, obtaining [26]:

$$J_{eff}(t) = \frac{4}{3}\frac{R^{\frac{1}{2}}}{P_0} h(t)^{\frac{3}{2}} \quad (12)$$

In case of soft materials where $E' \gg E$, the contact creep compliance becomes:

$$J(t) = \frac{4}{3(1-\upsilon^2)}\frac{R^{\frac{1}{2}}}{P_0} h(t)^{\frac{3}{2}} \quad (13)$$

Finally, $J(t)$ can be fitted to classical lumped parameters rheological models (e.g. Generalised Maxwell model) to derive the viscoelastic constants (i.e. spring and dashpot values) describing the material mechanical behaviour [27].

Stress-relaxation

Stress-relaxation can be considered the dual of creep test. It consists of measuring the load relaxation over time in response to a constant step indentation input (h_0). Assuming $E' \gg E$, the relaxation modulus can be expressed as:

$$E(t) = \frac{3(1-\upsilon^2)P(t)}{4R^{1/2}{h_0}^{3/2}} \quad (14)$$

and can be eventually fitted to lumped models to derive viscoelastic constants as creep compliance [27]. Notably, in general $E(t) \neq 1/J(t)$ except for $t = 0$ where $E(0) = 1/J(0)$.

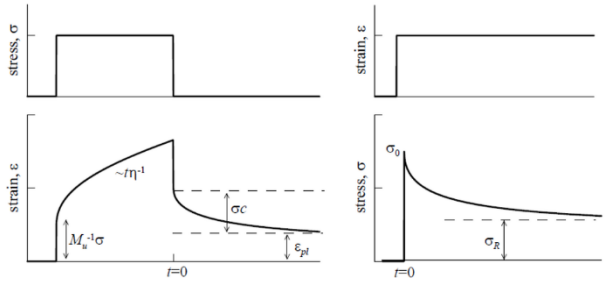

Figure 3 – Schematic representation of creep (left) and stress relaxation (right) including important parameters.

Nano-Dynamic Mechanical Analysis (nano-DMA)

Dynamic Mechanical Analysis (DMA) is a technique for viscoelastic characterization that has been applied in nanoindentation experiments for almost two decades. It is based on the application of a cyclic (sinusoidal) input of displacement or load with

frequency f and amplitude h_0 or P_0, respectively, and the measurement of the resultant load or displacement response. If the amplitude of the input oscillation is small enough, the measurements can be considered within the material Linear Viscoelastic Region (LVR), therefore the response obtained will be i) independent of the input amplitude, ii) sinusoidal with the same input frequency (f) and iii) with a phase lag ϕ. The latter is 0° for a purely elastic material, 90° for a purely viscous material, and in-between 0° and 90° for any viscoelastic material. Experimental data obtained for a given frequency can be used to compute the frequency-dependent storage (E') and loss (E'') moduli as per Eqn. 15 and 16 [28,29]:

$$\frac{E'(f)}{(1-v^2)} = \frac{P_0}{h_0} cos(\phi) \frac{1}{\sqrt{hR}} \quad (15)$$

$$\frac{E''(f)}{(1-v^2)} = \frac{P_0}{h_0} sin(\phi) \frac{1}{\sqrt{hR}} \quad (16)$$

Finally, frequency spectra of storage and loss moduli can be fitted to lumped parameter rheological models to derive material viscoelastic constants representing the mechanical behaviour as described in [17].

Nano-epsilon dot method (nano-$\dot{\varepsilon}$M)

Despite being largely used, the above mentioned techniques to characterise viscoelastic properties rely on the establishment of a small but measurable initial contact force to trigger load (creep) or displacement (stress-relaxation) step-input or the indenter oscillation, which may cause significant pre-stress and be detrimental to soft (bio)materials and biological tissues [1,17]. The nano-$\dot{\varepsilon}M$, stemming from the epsilon dot method ($\dot{\varepsilon}M$, [18]), allows to characterise material viscoelastic properties in absence of pre-stress through quick nano-indentation measurements performed at various constant strain rates starting $P-h$ acquisitions out of sample contact and without the need of any trigger force.

This method introduces new definitions of indentation stress and strain based on Hertz's contact model (Eqs. 12 and 13, respectively):

$$\sigma_{ind} = \frac{P}{R\sqrt{hR}} \quad (17)$$

$$\varepsilon_{ind} = \frac{4}{3(1-v^2)} \left(\frac{h}{R}\right) \quad (18)$$

which have several advantages, in particular:

- the ratio $\sigma_{ind}/\varepsilon_{ind}$ directly returns the sample modulus E (in case of fairly soft materials, where $E' \gg E$), without the need of any multiplicative factor;
- the constant indentation strain rate ($\dot{\varepsilon}_{ind}$) does not depend on the indentation h but only on the indenter velocity ($\dot{h}$). In fact, by using a constant indenter velocity, the displacement into surface is simply given by $h = \dot{h} \cdot t$ and consequently:

$$\dot{\varepsilon}_{ind} = \frac{\partial \varepsilon_{ind}}{\partial t} = \frac{4}{3(1-v^2)} \left(\frac{\dot{h}}{R}\right) = \text{constant during test} \quad (19)$$

Therefore, indentation stress and strain time-series at constant $\dot{\varepsilon}_{ind}$ required by the nano-$\dot{\varepsilon}M$ can be easily obtained by setting an appropriate indenter velocity ($\dot{h}$) to obtain the desired $\dot{\varepsilon}_{ind}$ according to Eq. 14. Then σ_{ind} and ε_{ind} can be calculated from experimental load (P) and displacement (h) data according to Eqs. 12 and 13, respectively. Subsequently, stress-time dataset obtained at different constant strain rates within the sample LVR (i.e. the region in which stress increases linearly with strain) can be globally fitted to a given lumped parameter rheological model to derive the viscoelastic constants describing the material mechanical behaviour, as reported in Tirella et al. [18].

4. References

[1] G. Mattei, A. Ahluwalia, Sample, testing and analysis variables affecting liver mechanical properties: A review, Acta Biomater. 45 (2016) 60–71. doi:10.1016/j.actbio.2016.08.055.

[2] M.L. Oyen, Nanoindentation of biological and biomimetic materials, Exp. Tech. 37 (2013) 73–87. doi:10.1111/j.1747-1567.2011.00716.x.

[3] G. Mattei, G. Gruca, N. Rijnveld, A. Ahluwalia, The nano-epsilon dot method for strain rate viscoelastic characterisation of soft biomaterials by spherical nano-indentation, J. Mech. Behav. Biomed. Mater. 50 (2015) 150–159. doi:10.1016/j.jmbbm.2015.06.015.

[4] J.L. Cuy, A.B. Mann, K.J. Livi, M.F. Teaford, T.P. Weihs, Nanoindentation mapping of the mechanical properties of human molar tooth enamel, Arch. Oral Biol. 47 (2002) 281–291. doi:10.1016/S0003-9969(02)00006-7.

[5] E. Gentleman, R.J. Swain, N.D. Evans, S. Boonrungsiman, G. Jell, M.D. Ball, T.A. V Shean, M.L. Oyen, A. Porter, M.M. Stevens, Comparative materials differences revealed in engineered bone as a function of cell-specific differentiation., Nat. Mater. 8 (2009) 763–70. doi:10.1038/nmat2505.

[6] S.E. Olesiak, M. Sponheimer, J.J. Eberle, M.L. Oyen, V.L. Ferguson, Nanomechanical properties of modern and fossil bone, Palaeogeogr. Palaeoclimatol. Palaeoecol. 289 (2010) 25–32. doi:10.1016/j.palaeo.2010.02.006.

[7] A. Karimzadeh, M.R. Ayatollahi, Mechanical properties of biomaterials determined by nano-indentation and nano-scratch tests, in: Nanomechanical Anal. High Perform. Mater., Springer, 2014: pp. 189–207.

[8] M.L. Oyen, Mechanical characterisation of hydrogel materials, Int. Mater. Rev. 59 (2013) 44–59. doi:10.1179/1743280413Y.0000000022.

[9] C. Albert, J. Jameson, J.M. Toth, P. Smith, G. Harris, Bone properties by nanoindentation in mild and severe osteogenesis imperfecta., Clin. Biomech. (Bristol, Avon). 28 (2013) 110–6. doi:10.1016/j.clinbiomech.2012.10.003.

[10] D.E. Ingber, Cellular mechanotransduction: putting all the pieces together again, FASEB J. 20 (2006) 811–827. doi:10.1096/fj.05-5424rev.

[11] G. Mattei, C. Ferretti, A. Tirella, A. Ahluwalia, M. Mattioli-Belmonte, Decoupling the role of stiffness from other hydroxyapatite signalling cues in periosteal derived stem cell differentiation, Sci. Rep. 5 (2015) 10778. doi:10.1038/srep10778.

[12] G. Mattei, C. Magliaro, S. Giusti, S.D. Ramachandran, S. Heinz, J. Braspenning, A. Ahluwalia, On the adhesion-cohesion balance and oxygen consumption characteristics of liver organoids, PLoS One. 12 (2017) e0173206. doi:10.1371/journal.pone.0173206.

[13] J.D. Kaufman, C.M. Klapperich, Surface detection errors cause overestimation of the modulus in nanoindentation on soft materials, J. Mech. Behav. Biomed. Mater. 2 (2009) 312–317. doi:10.1016/j.jmbbm.2008.08.004.

[14] G. Constantinides, K.S. Ravi Chandran, F.-J. Ulm, K.J. Van Vliet, Grid indentation analysis of composite microstructure and mechanics: Principles and validation, Mater. Sci. Eng. A. 430 (2006) 189–202. doi:10.1016/j.msea.2006.05.125.

[15] Y. Cao, D. Yang, W. Soboyejoy, Nanoindentation Method for Determining the Initial Contact and Adhesion Characteristics of Soft Polydimethylsiloxane, J. Mater. Res. 20 (2011) 2004–2011. doi:10.1557/JMR.2005.0256.

[16] J.D. Kaufman, G.J. Miller, E.F. Morgan, C.M. Klapperich, Time-dependent mechanical characterization of poly(2-hydroxyethyl methacrylate) hydrogels using nanoindentation and unconfined compression., J. Mater. Res. 23 (2008) 1472–1481. doi:10.1557/JMR.2008.0185.

[17] G. Mattei, A. Tirella, G. Gallone, A. Ahluwalia, Viscoelastic characterisation of pig liver in unconfined compression, J. Biomech. 47 (2014) 2641–2646. doi:10.1016/j.jbiomech.2014.05.017.

[18] A. Tirella, G. Mattei, A. Ahluwalia, Strain rate viscoelastic analysis of soft and highly hydrated biomaterials, J. Biomed. Mater. Res. Part A. 102 (2014) 3352–3360. doi:10.1002/jbm.a.34914.

[19] M.L. Oyen, R.F. Cook, A practical guide for analysis of nanoindentation data, J. Mech. Behav. Biomed. Mater. 2 (2009) 396–407. doi:10.1016/j.jmbbm.2008.10.002.

[20] W.C. Oliver, G.M. Pharr, An improved technique for determining hardness and elastic modulus using load and displacement sensing indentation experiments, J. Mater. Res. 7 (1992) 1564–1583. doi:10.1557/JMR.1992.1564.

[21] W.C. Oliver, G.M. Pharr, Measurement of hardness and elastic modulus by instrumented indentation: Advances in understanding and refinements to methodology, J. Mater. Res. 19 (2004) 3–20. doi:10.1557/jmr.2004.19.1.3.

[22] S. Pathak, S.R. Kalidindi, C. Klemenz, N. Orlovskaya, Analyzing indentation stress-strain response of LaGaO3 single crystals using spherical indenters, J. Eur. Ceram. Soc. 28 (2008) 2213–2220. doi:10.1016/j.jeurceramsoc.2008.02.009.

[23] J.S. Field, M.V. Swain, Determining the mechanical properties of small volumes of material from submicrometer spherical indentations, J. Mater. Res. 10 (1995) 101–112. doi:10.1557/JMR.1995.0101.

[24] I.N. Sneddon, The relaxation between load and penetration in the axisymmetric Boussinesq problem for a punch of arbitrary profile, Int. J. Eng. Sci. 3 (1965) 47–57.

[25] J.S. Field, M.V. Swain, A simple predictive model for spherical indentation, J. Mater. Res. 8 (1993) 297–306. doi:10.1557/JMR.1993.0297.

[26] H. Lu, B. Wang, J. Ma, G. Huang, H. Viswanathan, Measurement of Creep Compliance of Solid Polymers by Nanoindentation, Mech. Time-Dependent Mater. 7 (2003) 189–207. doi:10.1023/B:MTDM.0000007217.07156.9b.

[27] K.I. Schiffmann, Nanoindentation creep and stress relaxation tests of polycarbonate: Analysis of viscoelastic properties by different rheological models, Int. J. Mater. Res. 97 (2006) 1199–1211. doi:10.3139/146.101357.

[28] E.G. Herbert, W.C. Oliver, G.M. Pharr, Nanoindentation and the dynamic characterization of viscoelastic solids, J. Phys. D. Appl. Phys. 41 (2008) 74021. doi:10.1088/0022-3727/41/7/074021.

[29] H. van Hoorn, N.A. Kurniawan, G.H. Koenderink, D. Iannuzzi, Local dynamic mechanical analysis for heterogeneous soft matter using ferrule-top indentation, Soft Matter. 12 (2016) 3066–3073. doi:10.1039/C6SM00300A.